

Characterization of Epoxy Resin SU-8 Film Using Thickness-Shear Mode (TSM) Resonator

Lizhong Jiang, Jeanne Hossenlopp¹, Richard Cernosek², and Fabien Josse

Microsensor Research Laboratory and Department of Electrical and Computer Engineering, ¹Department of Chemistry, Marquette University, P.O. Box 1881, Milwaukee, WI 53201-1881, ²Micro-Analytical Systems Dept., Sandia National Laboratories, P.O. Box 5800, MS 0892, Albuquerque, NM 87185-0892

Abstract - Characterization of an organic resin (commonly known as SU-8), being investigated as waveguiding layer in the guided shear-horizontal surface acoustic wave (SH-SAW) sensor platforms, is presented. The impedance-admittance characteristics of the equivalent circuit models of both the unperturbed and coated resonators are analyzed to extract the storage modulus (G') and loss modulus (G''). The accuracy of the extracted shear modulus parameters occurs at high thickness where viscoelastic contribution is substantial. Apparently the polymer film is in a glassy state due to the high value of G' and high ratio of G' to G'' . Device resistance is less than 20 Ω when the thickness of film is less than 5 μm , beyond which viscoelastic properties significantly contribute to the frequency response. The extraction of the storage and loss moduli as a function of temperature ranging from -75 $^{\circ}\text{C}$ to 40 $^{\circ}\text{C}$ is also shown in order to study the effects of temperature on the shear modulus. Below -60 $^{\circ}\text{C}$, both the frequency shift and R_2 (the electrical resistance arising from the SU-8 film) are less dependent on temperature, which indicates that the polymer is almost totally elastic below -60 $^{\circ}\text{C}$. Exposure of SU-8 film to water and solutions of organic solvents such as acetone and ethanol also indicates, through frequency shift and resistance change, some degree of change in G' and G'' . However, stability is rapidly reached with exposure to DI water, indicating relatively lower water absorption.

I. INTRODUCTION

Thin polymer films are commonly used in the implementation of chemical and biochemical sensors, as partially selective and sensitive coatings for the detection of chemical agents [1-4], or as waveguiding layers in guided shear-horizontal surface acoustic wave (SH-SAW) sensor platforms [5]. The design and implementation of these sensors rely on the characteristic information about the viscoelastic properties of the polymer films and subsequent changes upon exposure to environmental factors, such as liquid contact and temperature change. Several technologies and techniques can be employed in characterizing the thin viscoelastic films. However, the use of the thickness-shear mode (TSM) quartz resonator is proposed here for rapid characterization because of its simplicity and ability to support shear horizontal waves, which are ideal for the characterization of the complex shear modulus of thin viscoelastic films.

The TSM resonator is very sensitive to surface perturbations. The surface perturbations include surface

mechanical loadings such as an ideal mass layer, a viscoelastic layer, and/or a contacting liquid. Two methods have been used to interpret TSM resonator response depending on the properties of perturbation: the Sauerbrey equation and the crystal impedance method. The Sauerbrey equation relates mass accumulated on the crystal to the change in the resonant frequency [6]. However, this method is only valid for a rigid and acoustically thin film. Since the mass effect is not the only effect that influences the acoustic behavior of the TSM device, the Sauerbrey method is unable to distinguish between changes in mass load on the surface and the viscosity changes of the liquid or changes in the viscoelastic properties of the coating. To overcome these limitations, the crystal impedance method has been developed [7-9]. This method allows the extraction of physical parameters (viscosity, density, shear modulus) from loading on the TSM resonator.

The TSM resonator consists of a thin disk of AT-cut quartz with metal electrodes deposited on both sides. Due to the piezoelectric properties and crystalline orientation of the quartz, application of alternating potential to the electrodes of the resonator results in an internal mechanical stress and consequently a shear deformation of the crystal. Resonance will occur when the crystal thickness is an odd multiple of half the acoustic wavelength. If a medium is in contact with one or both sides of the resonator surfaces, the excitation of the crystal subjects the medium on the crystal to an oscillatory driving force. Due to the electromechanical coupling, the mechanical properties of the contacting medium are reflected in the electrical response of the resonator.

The crystal impedance method involves using a network analyzer to measure the reflection coefficient, S_{11} of the surface-loaded TSM quartz resonator. From the reflection coefficient the admittance can be obtained in the form of complex quantities. It is convenient to use an equivalent circuit model to describe the electrical behavior of the TSM resonator. With only a few lumped elements, the modified Butterworth-VanDyke (BVD) model simulates the electrical characteristics of the TSM resonator over a range of frequencies near resonance. This model can explicitly relate the lumped elements in the circuit to physical properties of the TSM, as well as the surface loading (liquid load and/or viscoelastic film). Fitting the circuit model to the measured admittance data allows the extraction the physical properties of the surface perturbation [10].

II. THEORY

The modified BVD model can be used to describe the electrical response of the perturbed device. This model consists of two branches, see Fig. 1. A static capacitance C_0 arises between the electrodes located on opposite sides of the insulating quartz. A parasitic capacitance C_p arises due to the test fixture. Since the quartz is also piezoelectric, electromechanical coupling gives rise to an additional motional contribution (L_1 , C_1 and R_1). The static branch dominates the electrical behaviors away from resonance, while the motional branch dominates near resonance.

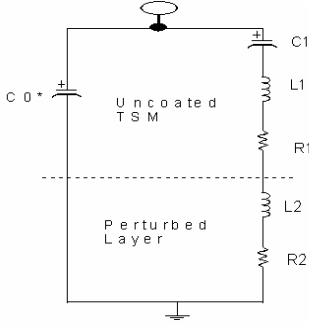


Fig. 1: Modified Butterworth-Van Dyke equivalent circuit of perturbed TSM resonator ($C_0^* = C_0 + C_p$)

When the resonator has a surface perturbation, the motional impedance contribution of this surface load is given by the complex electrical load impedance Z_e as [11]:

$$Z_e = \frac{N\pi}{4K^2\omega_s C_0} \left(\frac{Z_s}{Z_q} \right) \quad (1)$$

where N is the vibration mode index, K^2 is the square of the quartz electromechanical coupling coefficient, ω_s is the angular resonant frequency for the unperturbed TSM resonator, $Z_q = (\rho_q \mu_q)^{1/2}$ is the quartz shear wave characteristic impedance where ρ_q and μ_q are the mass density and shear stiffness of the quartz. Z_s is the shear mechanical impedance at the device surface [12]:

$$Z_s = \frac{T_{xy}}{v_x} \bigg|_{y=0} \quad (2)$$

where T_{xy} is the peak sinusoidal steady state shear stress imposed on the contacting medium by the resonator and v_x is the resulting x -directed surface shear particle velocity. Z_s is a complex quantity. Letting $Z_e = R_2 + j\omega L_2$, the electrical impedance element L_2 and R_2 can be related to the components of the surface mechanical impedance as:

$$R_2 = \frac{N\pi}{4K^2\omega_s C_0} \left(\frac{\text{Re}(Z_s)}{Z_q} \right) \quad (3.a)$$

$$L_2 = \frac{N\pi}{4K^2\omega_s C_0} \left(\frac{\text{Im}(Z_s)}{Z_q} \right) \quad (3.b)$$

A general model has been developed [13] which can incorporate a physically diverse set of single-component loading, including rigid solids, viscoelastic media, and fluids. In general, multiple surface loads on the TSM resonator cannot be treated in a linear fashion except for ideal mass layer. In case of TSM resonator with simultaneous viscoelastic and liquid loading, the total impedance is not equal to the sum of the characteristic impedance of the individual layers. This is due to the phase shift caused by the viscoelastic layer. Instead the total surface mechanical impedance is represented by:

$$Z_s^{\text{total}} = Z_0^{\text{film}} \left(\frac{Z_0^{\text{fluid}} \cosh(\gamma h_f) + Z_0^{\text{film}} \sinh(\gamma h_f)}{Z_0^{\text{film}} \cosh(\gamma h_f) + Z_0^{\text{fluid}} \sinh(\gamma h_f)} \right) \quad (4)$$

where Z_0^{film} is the characteristic mechanical impedance of a viscoelastic film, Z_0^{fluid} is the characteristic mechanical impedance of a Newtonian fluid, $\gamma = j\omega(\rho_f/G)^{1/2}$ is the complex wave propagation constant. ρ_f and h_f are the density and thickness of the film, respectively.

Polymer films are commonly applied as sorbing layers in gas and liquid-sensing applications. It is important to understand how the TSM resonator responds to the polymer coating. Polymers are viscoelastic materials and the elastic properties can be described by a complex modulus, $G = G' + jG''$. For the TSM loaded with a finite viscoelastic coating, the surface mechanical impedance Z_s seen at the resonator/film interface is derived from the transmission line theory and is given by [14]:

$$Z_s = jZ_0^{\text{film}} \tan \left(\omega_s \sqrt{\frac{\rho_f}{G}} h_f \right) \quad (5)$$

where Z_0^{film} is the characteristic impedance of the viscoelastic coating, given by $(\rho_f G)^{1/2}$. It is noted that when the TSM resonator is only loaded with a viscoelastic coating, equation (4) reduces to equation (5). The tangent function can be expanded in a Taylor series and the first three terms retained: $\tan(x) = x + x^3/3 + 2x^5/15$. This leads to: [3, 15, and 16]

$$\tan \left(\omega_s \sqrt{\frac{\rho_f}{G}} h \right) \approx \omega_s \sqrt{\frac{\rho_f}{G}} h + \frac{\omega_s^3 h^3 \rho_f^{3/2}}{3G^{3/2}} + \frac{2\omega_s^5 h^5 \rho_f^{5/2}}{15G^{5/2}} \quad (6)$$

The electrical impedance elements due to the viscoelastic layer can then be deduced from equation (1), (3), (4) and (6)

By setting $A = \frac{G''}{|G|^2}$ and $B = \frac{G'}{|G|^2}$, both the storage modulus G' and loss modulus G'' can be extracted as

$$G' = \frac{B}{A^2 + B^2} \quad (7)$$

$$G'' = \frac{A}{A^2 + B^2} \quad (8)$$

where

$$A = \left[\left(\frac{19\rho_f h}{24} - \frac{L_2}{A_0} \right) + \left[\left(\frac{L_2}{A_0} - \frac{19\rho_f h}{24} \right)^2 + \frac{R_2^2}{\omega_s^2 A_0^2} \right]^{\frac{1}{2}} \right]^{\frac{1}{2}} \quad (9)$$

$$\frac{4\omega_s^4 \rho_f^3 h^5}{15}$$

$$B = \frac{15R_2}{4\omega_s^5 \rho_f^3 h^5 A_0} \frac{1}{A} - \frac{5}{4\omega_s^2 h^2 \rho_f} \quad (10)$$

with

$$A_0 = \frac{N\pi}{4K_0^2 \omega_s C_0} \frac{1}{\sqrt{\mu_q \rho_q}} \quad (11)$$

III. EXPERIMENTAL

Polymer layers are spin-coated on the TSM resonators using SU-8-2002 solution. SU-8-2002 is used as received from MicroChem Corp. Processing of the SU-8 films involved exposure to UV light (15 minutes under 15W UV light) and two-step heating on a hot plate at 65°C and 95°C for two minutes each before and after the UV exposure. “Cured” SU-8 films are here defined as those which are put in an oven and heated at 200 °C for one hour after the preliminary processing described above. Multiple coatings are used to obtain a range of film thickness up to 22 μm. Determination of the thickness is very critical for accurate extraction of the shear moduli. A profilometer (α-step 100) is used to determine the thickness of each SU-8 film. The measured thickness from the profilometer concurs with the calibration of thickness vs. spin coating conditions as provided by the manufacturer.

A device of 9-MHz fundamental frequency is used in the study. Clean and uncoated TSM resonators are first characterized on the network analyzer to determine the equivalent circuit parameters for the unperturbed device near the resonance. Impedance is measured at the fundamental resonance frequency as well as the 3rd harmonic frequencies. R_1 , L_1 and C_1 and C_p can be obtained at this stage by fitting the experimental electrical impedance with the theoretical model of unperturbed TSM device (with $R_2=0$ and $L_2=0$ in Fig. 1). These parameters for the unperturbed device are stored for later use. Once thin films are spin-deposited, further measurements are gathered for the reflection coefficients, from which the impedance can be derived.

Experimentally obtained impedance data and film thicknesses are then used in the analysis. The density of the SU-8 film ρ_f is taken to be 1.2 g/cm³, as provided by the manufacturer. The analysis is then performed for the extraction of the shear moduli as indicated by equations (7-

11). Modeling of viscoelastic films involves finding the solutions to five parameters (G' , G'' , h_f , ρ_f and C_p). The parasitic capacitance C_p is included for the fact that C_p is closely related to the supporting structure which may change substantially after the coating. However, admittance measurements contribute only two parameters, real and imaginary part of mechanical impedance $Re(Z_s)$ and $Im(Z_s)$. We separate ρ_f out by equating the film density with that of the bulk value and h_f by our measurement results of profilometer. Both h_f and ρ_f are used as constraints in the modeling programs. Usually a tight constraint on h_f and ρ_f can generate unique solutions of G' and G'' .

A coated TSM resonator is put in an oven and connected to the Network Analyzer via a SMA connector and coaxial cable for the temperature-dependence studies. A thermal couple is attached in contact with the measurement cell for accurate control of temperature. For the investigation of the polymer film in liquid environments, a solution is injected into the measurement cell using a glass pipette. Ethanol and acetone (Aldrich, analytical grade) are used as supplied from the manufacturer. The resonant frequency and the admittance at the resonant frequency are recorded as a function of time after exposure to the liquids.

IV. RESULTS AND DISCUSSION

The resistance of the device (including the TSM resonator and SU-8 film) is shown in Fig. 2 for devices coated with SU-8 films of varying thickness. The resistance here represents the mechanical energy dissipation due to the surface load and the quartz crystal. Resistance remains very low (less than 20 ohm) when the thickness of the films is less than 5 μm. Beyond 5 μm the resistance increases sharply at first and then gradually approaches a maximum value. The resonant frequency of the coated device shifts to lower values as the coating thickness increases (see Fig. 3). When the thickness of the SU-8 film reaches 5 μm, the resonant frequency shift of the device apparently begins to deviate from the linear region and approaches the nongravimetric regime. This means that the viscoelastic properties of the polymer contribute to the device response and that significant deformation occurs on the upper film surface. The importance of contribution of viscoelastic properties increases as film thickness increases.

The dynamical behavior of the film's displacement across the thickness h_f is determined by the acoustic phase shift, ϕ , across the film. If the film is sufficiently thin and rigid so that $\phi < \pi/2$, then the entire film tends to move synchronously with the resonator surface and no strain (proportional to the displacement gradient) occurs in the film. The polymer film deformation is negligible only when the thickness of the film is much thinner than the acoustic wavelength. Beyond that range, the relation between the frequency shift and the mass loading is nonlinear because the acoustic delay in the overlay is no longer negligible [1, 14].

In the case of the SU-8 coated device, the phase velocity across the polymer film can be estimated as follows:

$$\nu = \left(\frac{G}{\rho} \right)^{1/2} \approx \left(\frac{1.6 \times 10^{10} \text{ dyne/cm}^2}{1.2 \text{ g/cm}^3} \right)^{1/2} \approx 1.16 \times 10^5 \text{ cm/s}$$

Using the value of shear modulus, $G = 1.6 \times 10^{10} \text{ dyne/cm}^2$ from our experimental results and the film density $\rho = 1.2 \text{ g/cm}^3$, the phase shift ϕ across the layer of $5 \mu\text{m}$ polymer film is:

$$\phi = 2\pi f h / \nu \approx 2\pi \times 9 \times 10^6 \times 5 \times 10^{-4} / (1.16 \times 10^5) \approx 0.077\pi < \frac{\pi}{2}$$

Therefore, a linear relationship between frequency shift and film thickness is observed in the approximate range of $0\text{--}5 \mu\text{m}$, beyond which viscoelastic properties will begin to more significantly contribute to the frequency response.

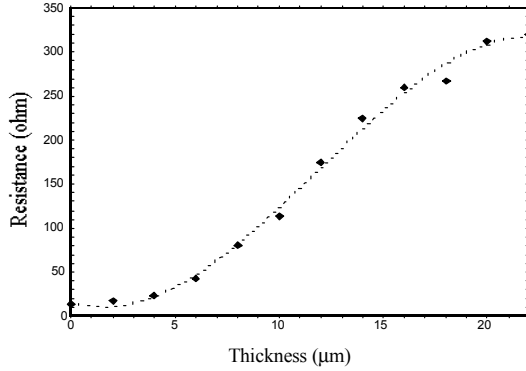


Fig. 2 The device resistance due to polymer coating and quartz crystal as a function of the thickness of SU-8 film. The device is a 9-MHz TSM resonator

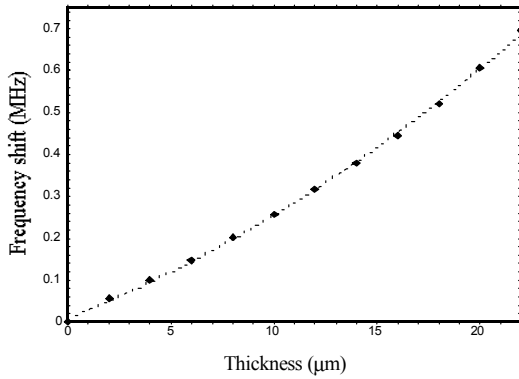


Fig. 3 Measured series-resonant frequency shifts as a function of the thickness of SU-8 film.

Film resonance occurs when $\phi = \pi/2$ ($h_f \approx 30 \mu\text{m}$). Film resonance represents the strongest coupling between the resonator and the coated film, resulting in a greater extraction of acoustic energy from the resonator. Resistance reaches its maximum at film resonance. The resistance change as a function of the film thickness (refer to Fig. 2) concurs with the plots reported by Martin and Frye [14]. The resistance is approaching but has not reached the maximum value at the thickness of $22 \mu\text{m}$. This result is quite consistent with our prediction that the film resonance occurs at $h_f \approx 30 \mu\text{m}$. Furthermore, it verifies the reliability of our fitting results of the shear modulus (G) for the SU-8 film.

The Sauerbrey equation indicates that the frequency shift is proportional to the square of the fundamental frequency of the TSM resonator. Therefore, the sensitivity/resolution of the device may be improved by operating the TSM resonator at higher odd harmonics. The use of multiple odd harmonics also allows one to solve the problem of uniqueness of fit for the viscoelastic films on TSM resonator. When the film density and thickness are not available, a unique solution will not be obtained if the crystal impedance measurements are made only at the fundamental frequency. By measuring the electrical response of the TSM resonator at various harmonics, more input variables are introduced.

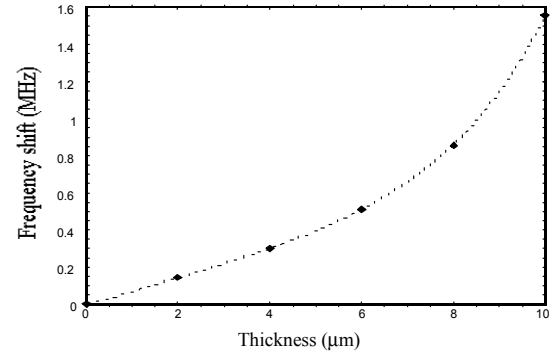


Fig. 4 The frequency shift of a coated device as a function of film thickness measured at third harmonic

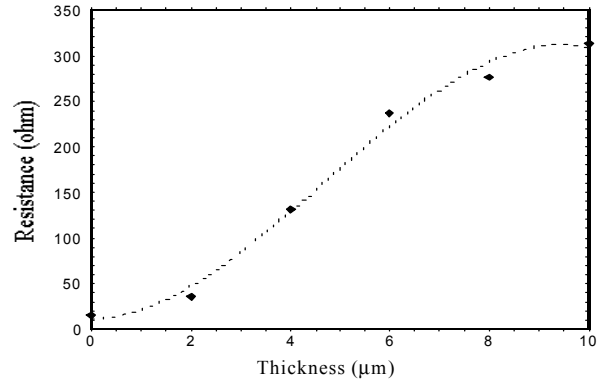


Fig. 5 The resistance (including the film and the resonator) as a function of film thickness measured at third harmonic

Figs. 4 and 5 show the frequency shift and loss of the TSM resonator with respect to the film thickness measured at the third harmonic. Compared to Fig. 3, the frequency shift of the third harmonic increases much faster than that of the fundamental frequency. Both the frequency shift and the resistance of the third harmonic for a film of thickness h are very close to that of the fundamental frequency for a film of a thickness $3h$. In Fig. 5, the device resistance approaches saturation at a thickness of approximately $10 \mu\text{m}$, agreeing with the prediction that the film resonance occurs at thickness around $10 \mu\text{m}$ for the third harmonic.

Measurements made at the fundamental frequency for the 9-MHz device are used to extract the shear moduli, G' and G''

and the results are shown in Fig. 6. Two densities of the film are used in order to evaluate the effect of the density on the values of the shear moduli. Both the storage and loss modulus from the two densities change in a similar pattern except that the values of shear moduli from the density $\rho=1.2 \text{ g/cm}^3$ are higher than those from $\rho=1.0 \text{ g/cm}^3$. It must be pointed out that the assumption of the polymer thickness and density is one of major sources of error.

The moduli increase with film thickness and the shear storage modulus exceeds the shear loss modulus by more than an order of magnitude. As the thickness increases to $15 \mu\text{m}$, both the storage modulus (G') and loss modulus (G'') approach saturation indicating that the viscoelastic properties are now independent of thickness. A thicker film layer is desirable for this analysis because of the very small viscoelastic contribution resulting from a thin film layer. For a relatively small film layer thickness, the extracted viscoelastic properties do not reflect that of a bulk film material. This essentially means that the phase shift across the thin film layer is practically negligible. Under these conditions, the extraction of the storage and loss modulus could be inaccurate. These figures confirm earlier discussion that meaningful values of viscoelastic properties can only be obtained at sufficiently large polymer thicknesses.

The storage modulus (G') of the SU-8 film (assuming $\rho = 1.2 \text{ g/cm}^3$) approaches its saturation value of $1.66 \times 10^{10} \text{ dyne/cm}^2$ for relatively thicker films ($>20 \mu\text{m}$), while the loss modulus (G'') reaches its maximum at $6.0 \times 10^8 \text{ dyne/cm}^2$ in the same range of thickness. Apparently the polymer film is in a state close to a glassy state due to the high value of G' and high ratio of G' to G'' . The storage modulus of SU-8 is comparable to that of PMMA, which is reported to be $1.43 \times 10^{10} \text{ dyne/cm}^2$ at a thickness of $17.6 \mu\text{m}$ [16].

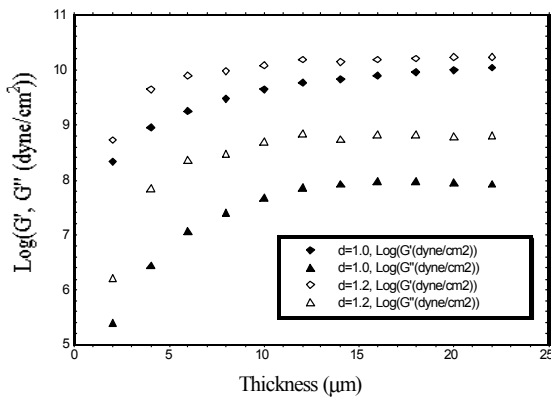


Fig. 6 Shear moduli as a function of the thickness of SU-8 film. Two densities are used for the extraction

Temperature is a significant environmental parameter that affects the performance of a TSM resonator. Figs. 7 and 8 show the device responses as a function of temperature in the range of $-75 \text{ }^\circ\text{C}$ – $40 \text{ }^\circ\text{C}$. In general, the device displays an initial rapid increase in resonant frequency shift when the temperature is decreased from $40 \text{ }^\circ\text{C}$ gradually until the

temperature is below $-60 \text{ }^\circ\text{C}$. Meanwhile, the device resistance decreases with decreasing temperature, with the smallest slope (smallest rate of change) at low temperatures. Since the bare crystal exhibits no change in response over this temperature range, the effects observed here should be mainly due to changes of the viscoelastic properties of the film.

Fig. 9 shows the device resistance as a function of temperature in the range of $-40 \text{ }^\circ\text{C}$ to $200 \text{ }^\circ\text{C}$. It is interesting to note that the device resistance increases with a decreasing

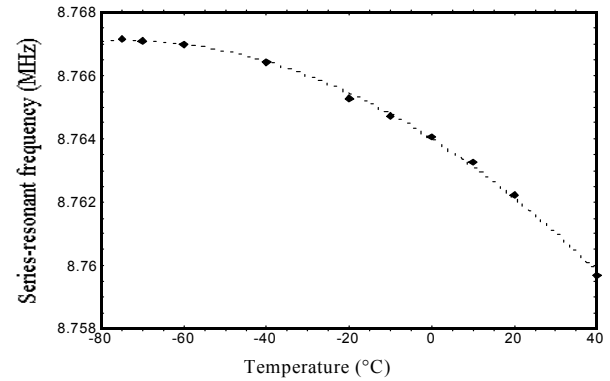


Fig. 7 Series-resonant frequency as a function of temperature for a device coated with $10 \mu\text{m}$ SU-8 film

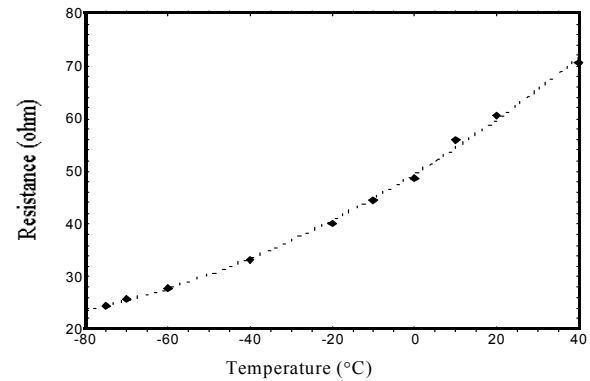


Fig. 8 Device resistance (including the film and the bare device) as a function of temperature in the range of $-75 \sim 40 \text{ }^\circ\text{C}$

temperature. This sharp change is due to the dramatic increase of the loss modulus G'' of the SU-8 film. The inflection point, which is located at around $180 \text{ }^\circ\text{C}$, may correspond to the glass transition temperature, T_g of the SU-8 film. Since no glass transition temperature T_g of SU-8 is available in the literature, this conclusion needs to be verified by other methods.

The process in which chemicals become associated with a solid phase is generally referred to as sorption (either adsorption onto the surface or absorption into the three-dimensional matrix). The sorption process is extremely important for the study of chemical sensors because it actually governs the outcome of the sensing process. The major effects of solute absorption by a polymer are swelling and

plasticization. The shear moduli of a SU-8 film in water are extracted based on a nonlinear multiple-loading model for a 10 μm SU-8 film. Since the SU-8 film is relatively thick and cannot be treated as an ideal mass layer, equation (4) should be used for the calculation of total impedance of the surface overlayers. The fitting results show that G' changes from 3.8×10^9 dyne/cm² to 1.75×10^9 dyne/cm² and G'' changes from 3.8×10^7 dyne/cm² to 1.1×10^8 dyne/cm² for an SU-8 film at a thickness of 10 μm . These results indicate that, upon exposure to DI water and water absorption, the film has become more viscoelastic. The thickness and density of the SU-8 film are assumed unchanged in the fitting program. One reason for this approximation is that SU-8 is a rigid film with high degree of crosslinking. The accuracy of these extracted shear moduli values need to be verified by other techniques.

Fig. 10 shows preliminary results of experiments conducted on a TSM device coated with a 1.5 μm SU-8 film upon exposure to various solutions. The results clearly show that acetone and ethanol solutions causes a greater response than DI water and the sensor responses increase with increasing concentration of the organic analyte in aqueous solutions. From Fig. 10, both ethanol and acetone have a stronger interaction with the SU-8 film than water and the ethanol has the strongest interaction of the three.

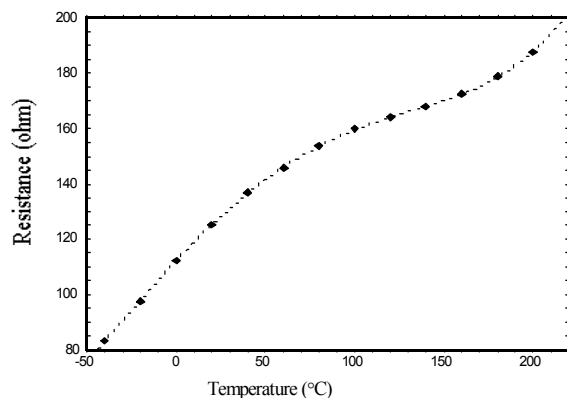


Fig. 9 Measured device resistance as a function of temperature for a device coated with 16 μm SU-8 film

Note that the relatively thin film may have also contributed to the observed results. The use of a thicker film, 10 μm , together with the liquid load resulted in a severe decrease of the device quality factor, Q , thus making measurements less accurate. It is also observed that, with the DI water load, the coated device has rapidly reached stability/saturation. This indicates a lower water uptake and/or a minimum effect on the viscoelastic properties of the coating.

V. CONCLUSIONS

The TSM quartz resonator has proven to be an effective tool in the characterization of polymer films under various conditions. Such studies are especially useful in the selection of appropriate polymers for the implementation of chemical

sensors in liquid environments and in the analysis of sensor stability under various conditions. The results for the SU-8 films indicate that the storage and loss moduli can be extracted with good accuracy at high thickness. Apparently the polymer film is in a near glassy state due to the high value of G' and high ratio of G' to G'' . A “plasticizing” effect is observed for the SU-8 film when exposed to solutions of some organic solvents. It is found that the polymer is almost totally elastic below -60°C .

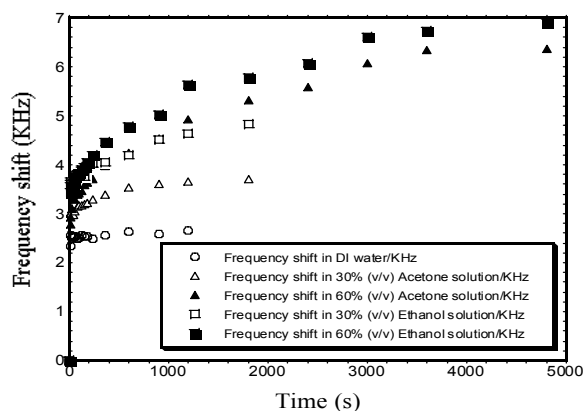


Fig. 10 Frequency shift as a function of time for a device coated with 1.5 μm SU-8 in liquid phase

ACKNOWLEDGMENT

This work is partially supported by NSF grant Nos: ECS-9876366, ECS-0110381 and CHE-0074962.

REFERENCES

- [1] D. S. Ballantine, R. M. White, S. J. Martin, et al., “*Acoustic wave sensors: theory, design, and physio-chemical applications*”, Academic Press: San Diego, 1997
- [2] G. Harsanyi, “Polymer films in sensor applications: a review of present uses and future possibilities”, *Sensor Review*, 2000, vol. 20, Number 2, pp. 98-105
- [3] R. M. Patel, R. Zhou, K. Zinszer, and F. Josse, “Real-time detection of organic compounds in liquid environments using polymer-coated thickness shear mode quartz resonators”, *Anal. Chem.* 2002, vol. 72, pp. 4888-4898
- [4] D. T. Hoa, T. N. Suresh Kumar, N. S. Punekar, R. S. Srinivasa, et al; “Biosensor based on conducting polymer”, *Analytical Chemistry*, 1992; vol. 64, Iss. 21; pp. 2645
- [5] F. Josse, F. Bender and R. W. Cernosek, “Guided SH-SAW sensor for chemical and biochemical detection in liquid”, *Anal. Chem.*, 2001, vol. 73, pp. 5937-5944
- [6] G. Z. Sauerbrey, “The use of quartz oscillators for weighing thin layers and for microweighing”, *Zeitschrift fuer physik.* 1959, vol. 155, pp. 206-222
- [7] E. Benes, “Improved quartz crystal microbalance technique”, *J. Appl. Phys.*, 1984, vol. 56, pp. 608
- [8] Y. Lee, Z.A. Shana, and F. Josse, “Quartz crystal Resonators as sensors in liquids using the acoustoelectric effect”, *Proceedings of the IEEE Ultrasonics Symposium, France*, 1994, pp. 633-638
- [9] S. J. Martin, G. C. Frye, and K. Wessendorf, “Sensing liquid properties with thickness-shear mode resonators”, *Sensors and Actuators A*, 1994, vol.44, pp. 209-218

- [10] S. J. Martin, V. E. Granstaff, and G. C. Frye, "Characterization of a quartz crystal microbalance with simultaneous mass and liquid loading", *Anal. Chem.*, 1991, vol. 63, pp. 2272-2281
- [11] S. J. Martin, G. C. Frye, A. J. Ricco and S. D. Senturia, "Effect of surface roughness on the response of thickness-shear mode resonators in liquids", *Anal. Chem.* 1993, vol. 65, pp. 2910-2922
- [12] W. G. Cady, *Piezoelectricity*, McGraw-Hill, New York, 1946
- [13] H. L. Bandey, S. J. Martin, and R. W. Cernosek, "Modeling the responses of thickness-shear mode resonators under various loading conditions", *Anal. Chem.*, 1999, vol. 71, pp. 2205-2214
- [14] S. J. Martin and G. C. Frye, "Polymer film characterization using quartz resonators", *Ultrasonic. Symp.* 1991, pp. 393-398
- [15] O. Wolff, E. Seydel and D. Johannsmann. "Viscoelastic properties of thin films studied with quartz crystal resonators", *Faraday Discuss. Chem. Soc.* 1997. vol. 107, pp. 91-104
- [16] B. Morray, S. Li, J. Hossenlopp, R. W. Cernosek, and F. Josse, "PMMA polymer characterization using thickness-shear mode (TSM) quartz resonator", *Proc. IEEE Freq. Cont. Symp and PDA Exhibition., New Orleans, LA* , 2002, pp. 294-300